

PAPER • OPEN ACCESS

Detection of Jacket Offshore Wind Turbine Structural Damage using an 1D-Convolutional Neural Network with a Support Vector Machine Layer

To cite this article: Christian Tutivén *et al* 2022 *J. Phys.: Conf. Ser.* **2265** 032088

View the [article online](#) for updates and enhancements.

You may also like

- [Analysis of students' difficulties about work and energy](#)
L Rivaldo, M R A Taqwa, A Zainuddin et al.
- [Asymmetric power consumption in rural electric networks](#)
I V Naumov, D N Karamov, A N Tretyakov et al.
- [Self-Curing Concrete Using Water-Soluble Polymer for Developing Countries](#)
T Udayabanu, N P Rajamane, C Makendran et al.



The Electrochemical Society
Advancing solid state & electrochemical science & technology

242nd ECS Meeting

Oct 9 – 13, 2022 • Atlanta, GA, US

Early hotel & registration pricing ends September 12

Presenting more than 2,400 technical abstracts in 50 symposia

The meeting for industry & researchers in

BATTERIES
ENERGY TECHNOLOGY
SENSORS AND MORE!



Register now!



ECS Plenary Lecture featuring
M. Stanley Whittingham,
Binghamton University
Nobel Laureate –
2019 Nobel Prize in Chemistry



Detection of Jacket Offshore Wind Turbine Structural Damage using an 1D-Convolutional Neural Network with a Support Vector Machine Layer

Christian Tutivén¹, Sueanny Moreno¹, Yolanda Vidal^{2,3}, and Carlos Benalcázar⁴

¹ESPOL Polytechnic University, Escuela Superior Politécnica del Litoral, Faculty of Mechanical Engineering and Production Science (FIMCP), Mechatronics Engineering, Campus Gustavo Galindo Km. 30.5 Vía Perimetral, P.O. Box 09-01-5863, Guayaquil, Ecuador

²Control, Modeling, Identification and Applications (CoDALab), Department of Mathematics, Escola d'Enginyeria de Barcelona Est (EEBE), Universitat Politècnica de Catalunya (UPC), Campus Diagonal-Besós (CDB), Eduard Maristany, 16, 08019 Barcelona, Spain

³Institute of Mathematics (IMTech), Universitat Politècnica de Catalunya (UPC), Pau Gargallo 14, 08028 Barcelona, Spain

⁴Universidad ECOTEC, Km. 13.5 Vía a Samborondón - Guayaquil, Ecuador

E-mail: cjtutive@espol.edu.ec, sgmorono@espol.edu.ec, yolanda.vidal@upc.edu, carlosbenalcazarparra@gmail.com

Abstract. Because offshore wind turbines, particularly their foundations, operate in hostile environments, implementing a structural health monitoring system is one of the best ways to monitor their condition, schedule maintenance, and predict possible fatal failures at lower costs. A novel strategy for detecting damage in offshore wind turbine jacket foundations is developed in this work, based on a vibration monitoring methodology that reshapes the data into a multichannel array, with as many channels as correlated sensors with the predicted variable, a 1-D deep convolutional neural network to extract temporal features from the monitored data, and a support vector machine as a final classification layer. The obtained model allows the detection of three types of bar states: healthy bar, cracked bar, and bar with an unlocked bolt.

1. Introduction

The planet's temperature has increased by 1.1 °C since 1850-1900, and the average global temperature is expected to reach or exceed an increase of 1.5 °C over the next 20 years (1). This increase is due to the massive emission of greenhouse gases, mainly from the burning of fossil fuels, which accounts for 75% of total emissions. In recent decades, many efforts have been made to promote the use of renewable energy to mitigate the effects of climate change. Options include solar, hydroelectric, geothermal, biofuels, biomass, and wind power. The importance of wind over other types of energy could be justified by analyzing three factors: resource availability, environmental impact, and cost-efficiency (2). In the last year, there was an increase of 93 GW of energy produced by wind turbines (WTs), accumulating a total of over 742,689 MW by the end of 2020. The highest growth of onshore WT installations equivalent to 95.25% takes



place in China and the USA with 56.30% and 19.46% respectively. While offshore installations equivalent to 4.75% are in China and the Netherlands with 50.45% and 24.62% respectively (3). Since 2015 there has been a considerable increase in offshore installations (1). Although they require a higher cost of installation and maintenance, they provide a more reliable and efficient energy generation because, unlike onshore installations, they have a better quality of wind resources since the wind is constant, has higher speeds and is more uniform, which reduces the fatigue of the structure and can increase the useful life of the generator (4). However, it also has some disadvantages, the main one being the high cost for offshore operations, in addition to the need to build or reinforce long electrical grids; another disadvantage is the advanced technology required for the development of wind farms, especially for the design of turbine foundations, which can be fixed or floating, but must be strong enough to adapt to the marine environment, withstanding corrosion conditions, high loads, fatigue and turbulence, some main causes of structural damage (5). Consequently, many studies are currently underway to analyze how to reduce these costs. One solution to this problem is the use of structural health monitoring (SHM) methodologies. The purpose of this method is to evaluate and monitor the structural health of the support structure in order to detect and predict the presence of damage, so the operational personal can take or plan actions.

There are different SHM techniques used for WT foundations, which have been developed over time to ensure reliability and efficiency in these systems. Among the main techniques are: Acoustic emission monitoring (6), thermal imaging (7), ultrasonic methods (8), fatigue and nodal properties monitoring (9), vibration deformation monitoring (10), and statistical pattern recognition (5). One of the techniques that has gained a lot of interest in recent years is statistical pattern recognition, which by implementing algorithms that can be supervised or unsupervised can monitor the health of structures (11; 12). The supervised learning approach is good for this application since, by having truthful information about the failure diagnosis, it will be possible to classify them during structural state monitoring reliably. This technique requires a large amount of data, as it must not only consider the healthy structural state of the foundation, but also all possible damages that you want to classify. Obtaining this information from an actual working structure would be very difficult or impossible to obtain. Therefore, a viable and widely used alternative is to obtain data from finite element analysis (FEM) which must be validated with a scale mode (13). This technique is applied in the present work, for which a WT laboratory-scale jacket-type structure is used, subjected to various types of failures and different vibrations, simulating its possible operating conditions, so it is considered a valid model.

The remainder of this paper is organized as follows. The experimental setup is introduced in Section 2. In Section 3 the proposed methodology and the 1D-convolutional neural network (CNN) with a support vector machine (SVM) classification layer are explained. The obtained results are given and discussed in Section 4. Finally, conclusions are drawn in Section 5.

2. Experimental Setup

For the present research, a scaled structure of a real jacket WT is used, see Figure 1. This model has a height of 2.7 m and consists of a jacket base, a tower and the nacelle. As it well known, WTs operate in three separate operating areas, depending on the wind speed. Because the losses are more than the electricity provided by the wind, the WT does not operate in region 1 because the wind speed is low. The wind speed in region 2 ranges between the cut-in and rated wind speeds. In this region, the major control goal is to maximize power production. Finally, the wind speed in region 3 is higher than the rated speed but lower than the cut-out wind speed. The key control goal in this region is to keep the produced power at the same level as the rated power (14). In this work, with the intention of simulating different wind regions (different wind speeds), the experiments consisted of generating four different frequencies of white noise to which

the gondola is exposed. Additionally, throughout the structure, eight tri-axial accelerometers are deployed to acquire vibration measurements at different WT locations, see Figure 1 (right).

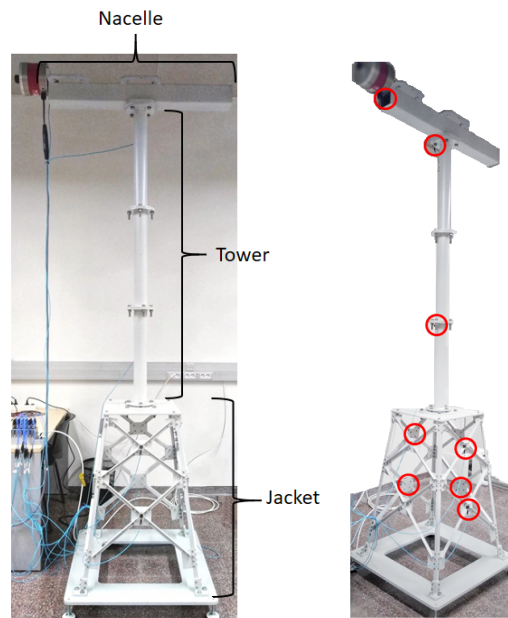


Figure 1. Scale structure with vibration sensors.

Moreover, the behavior of the structure is analyzed in three different structural states, related to one of the jacket bars located at level 2 of the wind turbine jacket structure, see Figure 2. One sort of deterioration encountered on offshore WT foundations is fatigue cracks. For small crack sizes, the chances of detecting a fatigue crack are slim. The crack growth rate, on the other hand, rises significantly for larger and thus more observable fatigue cracks. Consequently, there is only a small time window for detection and repair of this type of cracks before failure. Thus, in this work a 5 mm crack is one of the studied states. Please note that utilizing a similar laboratory tower model, a modal analysis and power spectral density signal processing algorithms were not able to detect this 5 mm crack located in the substructure in (15). The second studied state is the loosening of one of the jacket bolts. It is important to note that this damage is studied at level 2, which is submerged in water, so its detection is not visually evident. And finally the last studied state is when the bar is healthy (without damage). Figure 3, shows the three studied states (for more information, see (16)).

Finally, keep in mind that the goal of the study is to see if the proposed methodology has any practical application. The laboratory tower is a simplified model, but it is appropriate for this preliminary study because it is similar to the laboratory towers used in (15), where damage detection (but not localization or identification) is accomplished using damage indicators; in (17; 18), where statistical time series are used to detect damage; and in (19; 20), where damage detection is accomplished using principal component analysis and support vector machines.

3. Methodology

In this section, the proposed methodology is described. It is composed by the following steps: data acquisition, data split, feature selection, normalization, data reshape and, finally, the 1D-convolutional neural network with a support vector machine classification layer definition. Each of these stages are detailed below.

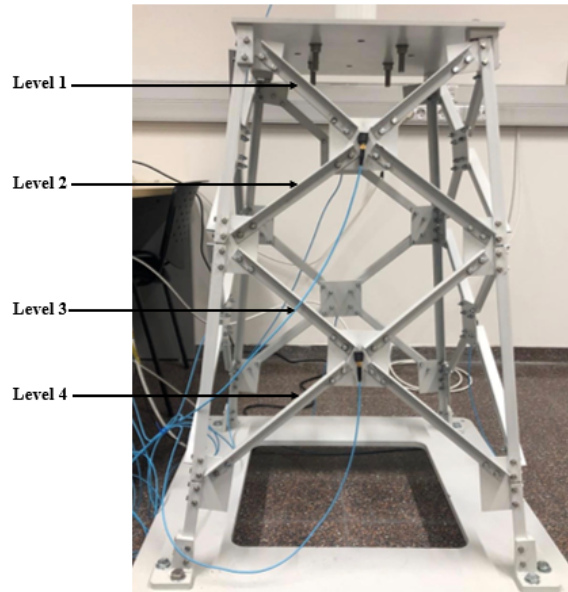


Figure 2. Location of the four levels at the jacket substructure. Level one is the closest to the surface and level four is the one submerged to a greater depth.



Figure 3. Different structural states of the studied bar. Healthy bar (**left**), cracked bar, where L is the length of the bar, $d = 5$ mm is the cracked size, and $X = L/3$ is the location of the crack in the bar (**center**), and unlocked bolt bar (**right**).

3.1. Data acquisition

The data used in the present work are composed of RMS vibration values obtained from eight tri-axial accelerometers deployed on the laboratory-scale jacket structure. The data obtained from the sensors is placed in the analysis dataset as one column for each coordinate, it means, for each sensor there are a total of three columns, so the study dataset has 24 columns of sensed values with the nomenclature shown in Table 1.

Table 1. Nomenclature of the variables used for analysis.

Sensor 1			. . .			Sensor 8		
x	y	z	.	.	.	x	y	z
s1x	s1y	s1z	.	.	.	s8x	s8y	s8z

A total of 80 experiments are performed, with a sampling frequency of 275.27 Hz, representing approximately 60 seconds of data acquisition for each experiment. For each analyzed state, several simulations were performed as shown in Table 2.

3.2. Data split: Train, validation and test sets

Each experiment consist of 16517, obtaining a total dataset of 1321360 samples. This dataset is divided into 80% for training data, 10% for validation data and 10% for testing, ensuring

Table 2. Total experiments performed for each frequency value and structural state analyzed.

No.	Structural state	White noise frequency [Hz]			
		0.5	1	2	3
1	Healthy bar	10	10	10	10
2	Cracked bar	5	5	5	5
3	Unlocked bar	5	5	5	5

complete samples for each experiment, as detailed in Table 3.

Table 3. Samples for each structural state used for training, validation and testing.

Structural State bar	Total of experiments	Samples for training	Samples for validation	Samples for testing	Total of samples
Healthy bar	40	528544	66068	66068	660680
Cracked bar	20	264272	33034	33034	330340
Unlocked bolt bar	20	264272	33034	33034	330340
Total	80	1057088	132136	132136	1321360

3.3. Feature selection

The correlation between the predictor variables and the variable to be predicted is analyzed. In this case, it represents all values obtained from sensors versus the predicted variable, which is called the class and refers to the structural state of the bar at the time of measurement. The correlation analysis made it possible to define the variables used in the subsequent data processing. Only those variables with a correlation factor greater than or equal to 0.15 or less than or equal to -0.15 with the variable to predict (state) are considered, since, according to the recommendation of (21). Table 4 lists all variables that are selected due to their high correlation.

Table 4. Selected variables after analyzing correlation between predictors and the predicted variable.

Selected sensors										
s1z	s2y	s2z	s3x	s3z	s4x	s4z	s5z	s6y	s7z	s8z

3.4. Data normalization

The data normalization process is essential in deep neural network applications, as it contributes to accelerating training and improving generalization capability (22). There are several techniques for data normalization, some of them are: z-score, Min Max, L1, L-infinity, histogram equalization, Mahalanobis distance and more. In this research is decided to use the Min Max method, which linearly rescales the data to an interval of [0,1] to change the values of the numerical columns by equivalent values in the delimited range, so that it uses a common scale maintaining the same distribution and proportion of the data without losing or distorting the information, in addition to helping the model in its processing (23). This operation is performed by the following Equation 1:

$$Y_j = \frac{X_j - x_{min_j}}{x_{max_j} - x_{min_j}}, \tag{1}$$

where j represents each column of the study data, this means a sensor coordinate correlated with the class.

$$x_{min_j} = \min(x_j), \quad \text{for } j = 1, \dots, 11, \tag{2}$$

and

$$x_{max} = \max(x_j), \quad \text{for } j = 1, \dots, 11. \tag{3}$$

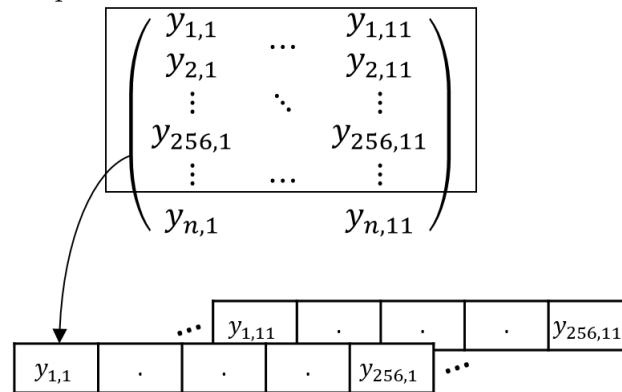
Using equation (1), the original matrix X , transforms to Y , which has the same dimensions but with normalized values.

3.5. Data Reshape

To prepare the data to use as an input to the CNN, it is decided to transform the normalized information from the sensors into a 1-dimensional multichannel image, to extract as many spatial-temporal characteristics of the data series as possible and, thus, to have a better classification (24).

As it is desired to create a model capable of classifying structural damage with the information of one second, sets of 256 values are taken to form the images (asthis corresponds approximately to one second of data acquisition). As this process is performed for each selected sensor, eleven vectors of 256 samples are obtained and grouped in a multichannel matrix, as occurs with three-channel RGB images. Finally, images with a dimension of 1 x 256 x 11 are obtained. A flowchart is given in Figure 4 where n represents the number of samples.

Figure 4. Reshape the clean and normalized data transformed into images.



Given the frequency of acquisition 64 images are generated from each experiment, it is important to note that great care was taken not to mix the remaining values from one experiment with another, thus discarding data from the last set of each experiment that were not large enough to become an image. Table 5 shows the total number of images generated for each data set.

Table 5. Number of images for each processing step.

	Training	Validation	Testing
No. of images	3584	768	768

3.6. 1D-Convolutional neural network

Deep CNNs have been widely used for the development of damage detection techniques in civil structures based on vibration measurements (25), (26). Recently, many studies that seek to analyze time series, where there are limited samples and the data usually present high variations or are acquired from different sources, as in this study, use 1D-CNN due to the advantages they offer including the compact configurations with fewer hidden layers, which reduces the number of parameters used and facilitates their training (27),(28),(29). Moreover, being compact, they consume less computational resources than a 2D-CNN, which makes them more economical and very viable for real-time analysis (30). Therefore, in this work, a 1D-CNN is used.

3.7. Support vector Machine classification layer

As is well known, there are multiple classification techniques in machine and deep learning, including feedforward neural networks, decision trees, K-nearest neighbor, Bayesian networks and SVM (31), (32). SVM is a technique based on the separation of the different classes of a training set by means of a surface that maximizes the margin between them, thus increasing their generalization capacity and, therefore, improving the classification capacity, thanks to which it has become popular in recent years and is considered superior to other techniques, especially when the data set is small, as in the case of this research (33). In this work, the usual feedforward classification layer in a CNN is replaced by an SVM classifier layer. To accomplish this, a multiple margin is used as the loss function (34). Additionally, the Adams algorithm is used as the optimizer, employing the following parameter: learning rate $\alpha_0=0.001$, beta values $\beta_1 = 0.9$, $\beta_2 = 0.999$, and $\epsilon = 10^{-8}$. Finally, a batch size of 16, with 25 training epochs are configured. In this work, two 1D-CNN with an SVM classification layer are trained to compare their results. The first one with only one convolutional layer and one max pooling layer (from now called 1D-CNN-V1), and the second with two convolutional layers and two max pooling layers (from now called 1D-CNN-V2). In Figure 5 and Table 6 can be observed the architecture of the 1D-CNN-V2, since it was the one that obtained the best performance.

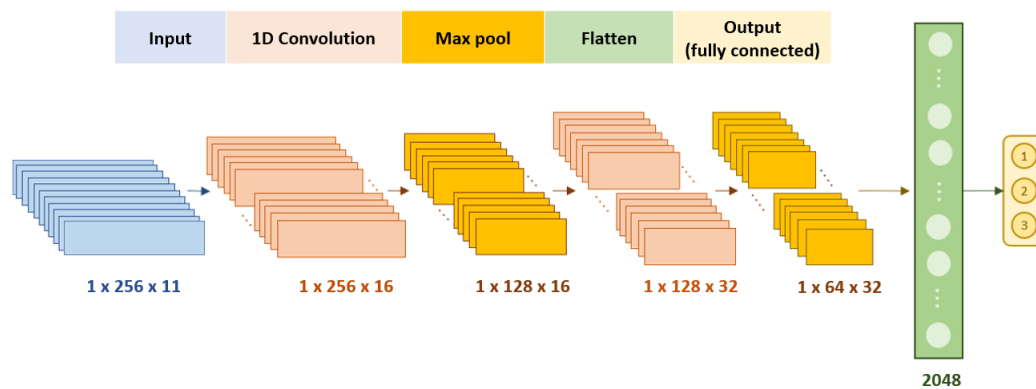


Figure 5. 1D-CNN-V2 architecture.

4. Results

As mentioned before, both networks are trained for 25 epochs, but the early stopping technique is used to save the best model (avoiding overfitting) and not the last trained one. Figure 6 shows the result of the 1D-CNN-V1 model. As can be observed, the best model is saved in the epoch number 15. On the left side of the figure, it can be seen that the model is overfitting since the validation loss is higher than the training loss. On the other hand, on the right side of the figure the confusion matrix is observed where it is evident that this model is not capable of

Table 6. Description of the 1D-CNN-V2 architecture.

Layer	Output size	Parameters	Number of parameters
Input 1 x 256 x 11 images	1x256x11	-	0
Convolution 16 Filters of size 3 with stride=1 & padding=1 ReLU	1x256x16	Weight 3x11x16 Bias 1x16	544 0
Max pool of size 3 with stride=2 & padding=1	1x128x16	-	0
Convolution 32 Filters of size 3 with stride=1 & padding=1 ReLU	1x128x32	Weight 3x16x32 Bias 1x32	1568 0
Max pool of size 3 with stride=2 & padding=1	1x64x32	-	0
Drop out (40%)	1x64x32	-	0
Fully connected #1	1x3	Weight 2048x3 Bias 1x3	6147
Class output	-	-	0

correctly classifying the cracked bar state. These results represent an accuracy of 89% on the test data set, which is equivalent to 684 correctly classified samples, out of 768, as seen in the confusion matrix. While for precision, recall, and F1 score, the values are 0.9065, 0.8906, and 0.8842, respectively.

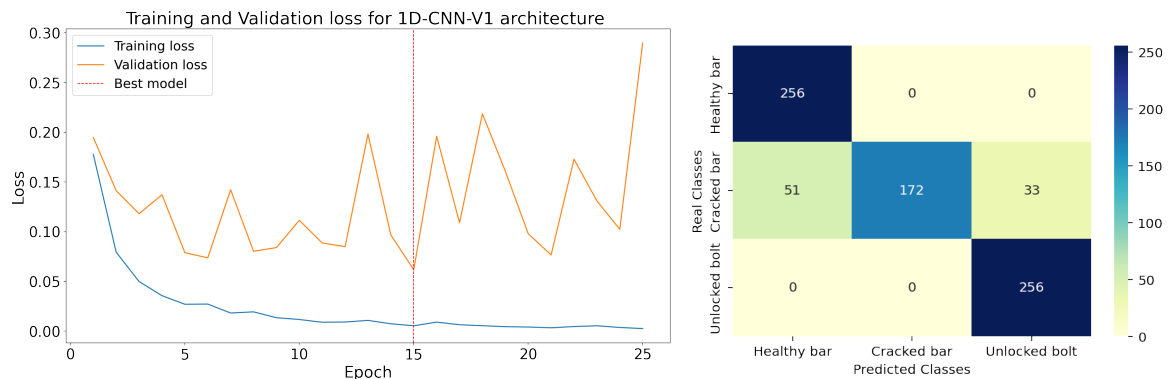


Figure 6. Validation and training loss (left) and confusion matrix (right) for the 1D-CNN-V1 model.

The second architecture (1D-CNN-V2) obtained the best model after 10 epochs. The results obtained by this model can be seen in Fig. 7. As can be observed on the left side of the figure, the best model is not overfitting since it has a lower validation loss compared to the training loss, which means the model generalizes well. The accuracy increases to 100% (see, right side of the figure), correctly predicting all cases. This shows how extracting more features with the 32 filters from the second convolutional layer helps to improve the classification.

Finally, to comprehensively verify the algorithm's functional properties, a comparison is done with four additional techniques that use the identical laboratory setup (19), (15), (35), and (16). The first method is based on principal component analysis and support vector machines, as described in (19). The second methodology is based on the well-known damage indicators: covariance matrix estimate and scalar covariance, as described in (15) (page 67).

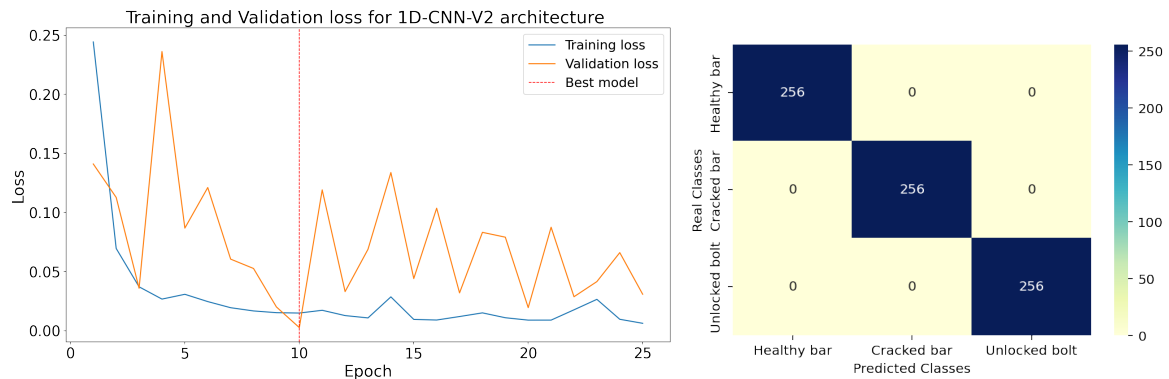


Figure 7. Validation and training loss (**left**) and confusion matrix (**right**) for the 1D-CNN-V2 model.

The third approach, described in (35), is based on machine learning and the fractal dimension characteristic. The final solution, described in (16), combines synthetic data augmentation with signal-to-image conversion of accelerometer data into multichannel pictures and convolutional neural networks (CNN). First, the crack damaged bar obtained using the first approach indicated in (19) has a recall of 96.08 percent, which is inferior to the one obtained using the strategy proposed in this study, which reached a value of 100 percent. It's worth noting that fracture damage is the most difficult to repair. In fact, utilizing scalar covariance or mean residual damage indicators, the second approach described in (15) (page 82) was unable to detect this form of incipient damage. Furthermore, the first method achieves a recall of 99.02 percent for unlocked bolt damage, but the recommended way achieves a little higher number of 100%. It's worth noting that the second approach ignores the unlocked bolt damage. The third approach (35) necessitates feature extraction by hand, and the performance measures produced are inferior to those in this study. Furthermore, the machine learning approaches presented in (35) require a big data set to get decent results, but Siamese neural networks can learn from very little data, which is critical in the application addressed in this paper. Finally, the fourth technique (16) necessitates a deep CNN as well as a 25,200% increase in the total number of samples to achieve 99 percent accuracy, whereas the proposed strategy achieves superior accuracy with far less data and a much simpler neural network architecture.

5. Conclusions

In this work, a strategy based on 1D-CNN with an SVM classification layer and based solely on vibration response is demonstrated for the structural health monitoring of offshore WT foundations. The methodology demonstrated exceptional performance by classifying three different bar states. The conceived SHM methodology with a deeper architecture shows exceptional performance, with all considered metrics (accuracy, precision, recall, F1-score, and specificity) giving results of 100%. These results show that large (deep) 1D-CNNs are promising for the development of SHM strategies for WT offshore foundations.

Because the data was gathered in a controlled laboratory context, this study is a proof-of-concept contribution. As a result, it is proposed that future research include other environmental factors, such as wave excitation, by setting up the experiment in a water tank facility to imitate the influence of regular and irregular waves. Finally, environmental and operational conditions (EOC) are vital to consider when dealing with long-term monitoring because they can make damage identification more difficult. Because of the wide range of EOCs, EOC monitoring is almost as critical as structural monitoring. As a result, its impact should be mitigated. To

make SHM possible, several approaches for EOC compensation for WTs have been devised. In (36), for example, affinity propagation clustering is utilized to divide data into WT groups with comparable EOC. Experimental covariance-driven stochastic subspace identification is utilized in (37). Finally, for EOC compensation, fuzzy classification approaches are utilized in (38) and (39). However, as previously said, this work is merely a proof of concept, actual EOC compensation will have to wait for further research employing pattern recognition techniques in a more realistic setting.

Acknowledgments

This work has been partially funded by the Spanish Agencia Estatal de Investigación (AEI)—Ministerio de Economía, Industria y Competitividad (MINECO), and the Fondo Europeo de Desarrollo Regional (FEDER) through the research project DPI2017-82930-C2-1-R; and by the Generalitat de Catalunya through the research project 2017 SGR 388.

References

- [1] Z. Zhongming, L. Linong, Z. Wangqiang, L. Wei *et al.*, “Climate change 2021: The physical science basis,” 2021.
- [2] M. D. Esteban, J. J. Diez, J. S. López, and V. Negro, “Why offshore wind energy?” *Renewable Energy*, vol. 36, no. 2, pp. 444–450, 2011.
- [3] G. W. E. Council, “Gwec— global wind report 2021,” 2021.
- [4] I. IRENA, “Future of wind: Deployment, investment, technology, grid integration and socio-economic aspects,” 2019.
- [5] M. Martínez-Luengo, A. Kolios, and L. Wang, “Structural health monitoring of offshore wind turbines: A review through the statistical pattern recognition paradigm,” *Renewable and Sustainable Energy Reviews*, vol. 64, pp. 91–105, 2016. [Online]. Available: <https://www.sciencedirect.com/science/article/pii/S1364032116301976>
- [6] G. Lapoutre, “Acoustic emission monitoring: of offshore wind turbine support structures for detection and localization of fatigue crack growth,” 2017. [Online]. Available: <http://resolver.tudelft.nl/uuid:a5d405b1-92a7-4320-af33-da94602d87ed>
- [7] H. Sanati, D. Wood, and Q. Sun, “Condition monitoring of wind turbine blades using active and passive thermography,” *Applied Sciences*, vol. 8, p. 2004, 10 2018.
- [8] F. P. García Marquez and C. Q. Gómez Muñoz, “A new approach for fault detection, location and diagnosis by ultrasonic testing,” *Energies*, vol. 13, no. 5, 2020. [Online]. Available: <https://www.mdpi.com/1996-1073/13/5/1192>
- [9] A. Iliopoulos, W. Weijtjens, D. Van Hemelrijck, and C. Devriendt, “Fatigue assessment of offshore wind turbines on monopile foundations using multi-band modal expansion,” *Wind Energy*, vol. 20, no. 8, pp. 1463–1479, 2017.
- [10] D. Ma, Y. Li, Y. Liu, J. Cai, and R. Zhao, “Vibration deformation monitoring of offshore wind turbines based on gbir,” *Journal of Ocean University of China*, vol. 20, no. 3, pp. 501–511, 2021.
- [11] T. Regan, C. Beale, and M. Inalpolat, “Wind turbine blade damage detection using supervised machine learning algorithms,” *Journal of Vibration and Acoustics*, vol. 139, 06 2017.
- [12] D.-A. Tibaduiza, M.-A. Torres-Arredondo, L. Mujica, J. Rodellar, and C.-P. Fritzen, “A study of two unsupervised data driven statistical methodologies for detecting and classifying damages in structural health monitoring,” *Mechanical Systems and Signal Processing*, vol. 41, no. 1-2, pp. 467–484, 2013.

- [13] S. Gopalakrishnan, M. Ruzzene, and S. Hanagud, "Application of the finite element method in shm," 07 2011.
- [14] L. Y. Pao and K. E. Johnson, "Control of wind turbines," *IEEE Control systems magazine*, vol. 31, no. 2, pp. 44–62, 2011.
- [15] E. Zugasti Uriguen, "Design and validation of a methodology for wind energy structures health monitoring," 2014.
- [16] B. Puruncajas, Y. Vidal, and C. Tutivén, "Vibration-response-only structural health monitoring for offshore wind turbine jacket foundations via convolutional neural networks," *Sensors*, vol. 20, no. 12, 2020. [Online]. Available: <https://www.mdpi.com/1424-8220/20/12/3429>
- [17] N. I. Spanos, J. S. Sakellariou, and S. D. Fassois, "Exploring the limits of the truncated sprt method for vibration-response-only damage diagnosis in a lab-scale wind turbine jacket foundation structure," *Procedia engineering*, vol. 199, pp. 2066–2071, 2017.
- [18] N. A. Spanos, J. S. Sakellariou, and S. D. Fassois, "Vibration-response-only statistical time series structural health monitoring methods: A comprehensive assessment via a scale jacket structure," *Structural Health Monitoring*, vol. 19, no. 3, pp. 736–750, 2020.
- [19] Y. Vidal Seguí, J. L. Rubias, and F. Pozo Montero, "Wind turbine health monitoring based on accelerometer data," in *9th ECCOMAS Thematic Conference on Smart Structures and Materials*, 2019, pp. 1604–1611.
- [20] Y. Vidal, G. Aquino, F. Pozo, and J. E. M. Gutiérrez-Arias, "Structural health monitoring for jacket-type offshore wind turbines: experimental proof of concept," *Sensors*, vol. 20, no. 7, p. 1835, 2020.
- [21] P. Schober, C. Boer, and L. Schwarte, "Correlation coefficients: Appropriate use and interpretation," *Anesthesia & Analgesia*, vol. 126, p. 1, 02 2018.
- [22] L. Huang, J. Qin, Y. Zhou, F. Zhu, L. Liu, and L. Shao, "Normalization techniques in training dnns: Methodology, analysis and application," 09 2020.
- [23] L. Friedman and O. V. Komogortsev, "Assessment of the effectiveness of seven biometric feature normalization techniques," *IEEE Transactions on Information Forensics and Security*, vol. 14, no. 10, pp. 2528–2536, 2019.
- [24] O. Avci, O. Abdeljaber, S. Kiranyaz, and D. Inman, "Structural damage detection in real time: implementation of 1d convolutional neural networks for shm applications," in *Structural Health Monitoring & Damage Detection, Volume 7*. Springer, 2017, pp. 49–54.
- [25] N. Pathak, "Bridge health monitoring using cnn," in *2020 International Conference on Convergence to Digital World-Quo Vadis (ICCDW)*. IEEE, 2020, pp. 1–4.
- [26] W. Weijtjens, T. Verbelen, E. Capello, and C. Devriendt, "Vibration based structural health monitoring of the substructures of five offshore wind turbines," *Procedia Engineering*, vol. 199, pp. 2294–2299, 2017, x International Conference on Structural Dynamics, EURO DYN 2017. [Online]. Available: <https://www.sciencedirect.com/science/article/pii/S1877705817336305>
- [27] S. Kiranyaz, T. Ince, and M. Gabbouj, "Real-time patient-specific ecg classification by 1-d convolutional neural networks," *IEEE Transactions on Biomedical Engineering*, vol. 63, no. 3, pp. 664–675, 2016.
- [28] O. Avci, O. Abdeljaber, S. Kiranyaz, M. Hussein, and D. J. Inman, "Wireless and real-time structural damage detection: A novel decentralized method for wireless sensor networks," *Journal of Sound and Vibration*, vol. 424, pp. 158–172, 2018.
- [29] O. Avci, O. Abdeljaber, S. Kiranyaz, and D. Inman, "Structural damage detection in real time: implementation of 1d convolutional neural networks for shm applications," pp. 49–54, 2017.

- [30] S. Kiranyaz, O. Avci, O. Abdeljaber, T. Ince, M. Gabbouj, and D. J. Inman, “1d convolutional neural networks and applications: A survey,” *Mechanical Systems and Signal Processing*, vol. 151, p. 107398, 2021. [Online]. Available: <https://www.sciencedirect.com/science/article/pii/S0888327020307846>
- [31] D. Srivastava and L. Bhambhu, “Data classification using support vector machine,” *Journal of Theoretical and Applied Information Technology*, vol. 12, pp. 1–7, 02 2010.
- [32] R. Colloca, A. E. Johnson, L. Mainardi, and G. D. Clifford, “A support vector machine approach for reliable detection of atrial fibrillation events,” pp. 1047–1050, 2013.
- [33] J. Cervantes, F. Garcia-Lamont, L. Rodríguez-Mazahua, and A. Lopez, “A comprehensive survey on support vector machine classification: Applications, challenges and trends,” *Neurocomputing*, vol. 408, pp. 189–215, 2020. [Online]. Available: <https://www.sciencedirect.com/science/article/pii/S0925231220307153>
- [34] Y. Tang, “Deep learning using linear support vector machines,” *arXiv preprint arXiv:1306.0239*, 2013.
- [35] E. Hoxha, Y. Vidal, and F. Pozo, “Damage diagnosis for offshore wind turbine foundations based on the fractal dimension,” *Applied Sciences*, vol. 10, no. 19, p. 6972, 2020.
- [36] M. W. Häckell, R. Rolfes, M. B. Kane, and J. P. Lynch, “Three-tier modular structural health monitoring framework using environmental and operational condition clustering for data normalization: Validation on an operational wind turbine system,” *Proceedings of the IEEE*, vol. 104, no. 8, pp. 1632–1646, 2016.
- [37] P. Kraemer, H. Friedmann, C. Ebert, J. Mahowald, and B. Wölfel, “Experimental validation of stochastic subspace algorithms for structural health monitoring of offshore wind turbine towers and foundations,” in *Proceedings of the 8th European Workshop On Structural Health Monitoring, Bilbao, Spain*, 2016, pp. 5–8.
- [38] C. P. Fritzen, P. Kraemer, and I. Buethe, “Vibration-based damage detection under changing environmental and operational conditions,” in *Advances in Science and Technology*, vol. 83. Trans Tech Publ, 2013, pp. 95–104.
- [39] W. Ostachowicz and A. Güemes, *New trends in structural health monitoring*. Springer Science & Business Media, 2013, vol. 542.